

Early Cosmic Chemical Evolution: Relating the Origin of a Diffuse Intergalactic Medium and the First Long-Lived Stars

F.D.A. Hartwick

*Department of Physics and Astronomy,
University of Victoria, Victoria, BC, Canada, V8W 3P6*

ABSTRACT

Nucleosynthetic signatures in common between the gas responsible for the high redshift Lyman α forest and a subsample of extremely metal poor stars are found. A simple mass loss model of chemical evolution with physically motivated parameters provides a consistent picture in which the gas is identified with that lost by supernova-driven winds during the first generation of star formation. Substantial mass loss occurs which can account for a diffuse IGM with up to 80% of the total baryon content and a peak [C-O/H] abundance of ~ -2.9 . This mass loss component differs from one produced later during galaxy formation and evolution that contributes to a circum-galactic medium (CGM). The CGM was shown earlier to have a mass of $\sim 10\%$ of all baryons and peak [Fe/H] ~ -1 .

Subject headings: intergalactic medium

1. Introduction

It is well known that the stellar content of the universe is only about $\sim 10\%$ of the total baryonic content (e.g. Fukugita & Peebles 2004). It is also well established that vigorous star formation, which occurs during galaxy formation and evolution, is accompanied by mass loss (e.g. Veilleux et al. 2005). According to some models this mass loss can account for another $\sim 10\%$ of all baryons (e.g. Hartwick 2004, hereafter H04). What is the origin and composition of the remaining $\sim 80\%$ of all baryons? This question is addressed here using recent observational data and simple chemical evolution arguments.

Generally the abundance distribution exhibited by stellar spectra reflects the material that formed the stars. If one were to observe spectra of the oldest stars (most metal poor?) in our Galaxy, then one expects to have to look at high redshifts in order to find gas with the same nucleosynthetic signature.

At redshifts of order 3, the baryon budget is believed to be dominated by the tenuous gas responsible for producing the Lyman α forest observed in absorption in high redshift quasar spectra (e.g. Rauch 1998). As discussed below, recent high quality data from the largest telescopes combined with sophisticated reduction techniques have allowed the detection of the heavy elements C, O, and Si in low column densities of hydrogen. These new observational results have prompted a re-examination of a possible connection between this gas and the earliest star formation (Pop III?) phase. By modelling the observed distribution of carbon or oxygen in this gas, we can predict the distribution of these elements and characteristic abundance ratios expected in long-lived stars, if they had been formed at the same early time. Unfortunately both the gas and stellar samples, are small and incomplete. Yet, we find encouraging consistency with the hypothesis when comparing these observations with the results from a simple, physically motivated, mass loss model of chemical evolution. An important and surprising conclusion is that long-lived stars with nucleosynthetic signatures in common with the Lyman α forest gas do exist.

2. The Observations

2.1. The Diffuse Gas

Early work on the detection of carbon in low column density Lyman α clouds was carried out by Cowie, Songaila, Kim & Hu (1995). More recently, Simcoe, Sargent & Rauch (2004) used survival analysis (a technique which makes use of non-detections as well as detections) to construct the distribution of [O/H] and [C/H] in low column density absorption lines along lines of sight to seven quasars. The data become incomplete at [O/H] \lesssim -3.0 (no floor was detected), but above that the distribution was log-normal with mean [C-O/H] ~ -2.85 and dispersion ± 0.75 , with these results depending on the assumed shape of the UV background (UVB). A second well fit model used a softer UVB resulting in medians of [C/H] ~ -3.1 and [O/H] ~ -2.7 . The ionizing UVB models are those of Haardt & Madau (1996) and are made up of contributions from a quasar continuum and a galaxy contribution. A softer spectrum implies more contribution from galaxies and less from quasars.

The information in Fig. 14 of Simcoe, Sargent & Rauch (2004) is the starting point for the present work. A second important observational constraint comes from Schaye et al. (2003) who determined the silicon to carbon ratio [Si/C] in the Lyman α forest down to very low column densities. They found this ratio to be ~ 0.77 , again depending on the shape of the UVB that is assumed, with a softer UVB (more galaxy and less quasar contribution) resulting in a lower [Si/C] ratio. The authors concluded that this [Si/C] ratio is unlikely to be lower than ~ 0.5 .

2.2. The Stellar Sample

When the chemical evolution model is constrained by observations of the diffuse gas, one can predict the [C-O/H] distribution in stars, assuming that luminous long-lived remnants were produced. Further, the stars should also show appropriate [Si/C] signatures. If such stars were formed, we can reasonably expect to find them among the various samples of extremely metal poor stars which have been spectroscopically analyzed. The data discussed below follows from earlier work by Gratton & Sneden (1988, 1991), McWilliam et al. (1995), Ryan, Norris & Beers (1996), and others.

Here we are concerned primarily with the abundances of C, O, Mg, Si, and Fe. Unfortunately, not all of these abundances are available from every study, and care must be exercised when interpreting and combining these results, since the samples are subject to strong observational selection effects. In addition, most of the work has been done on giant stars whose atmospheres are subject to non-LTE effects, possible mixing effects, 1-D versus 3-D effects, and incompleteness due to the weakness of lines analyzed. Carbon and oxygen are particularly vulnerable. Our main sources of data are the work of Cayrel et al. (2004) and a further discussion of the carbon and oxygen abundances of the same stars by Spite et al. (2005). For carbon [C/Fe], the sources are the unmixed stars of Spite et al. (2005), Akerman et al. (2004), as well as those stars from Honda et al. (2004) and Barklem et al. (2005) with $\log L/L_{\odot} \lesssim 2.3$ (calculated from $\log T_{eff}$, $\log g$, and assumed mass of $0.8 M_{\odot}$). This selection criterion was used in order to reduce the possibility of including mixed-CNO atmospheres. Note that all sources, except Barklem et al., avoided including carbon-rich stars. Data for oxygen [O/Fe] are from Akerman et al. (2004) and Spite et al. (2005). Following Spite et al., their [O/Fe] data were lowered by 0.25 dex to agree with the Akerman et al. data. Magnesium abundances [Mg/Fe] are available from all sources except Akerman et al., silicon [Si/Fe] from all sources except Akerman et al. and Barklem et al., while values of [Fe/H] are available for all stars.

Generally, the above samples contain some of the most metal poor stars known. Most of these stars are more metal poor than the metal poorest globular clusters ($[Fe/H] \sim -2.4$, $[O/H] \sim -1.8$). As such they are assumed to have comparable or older ages ($\sim 13 - 14 \times 10^9$ yrs) and hence masses $\sim 0.8 M_{\odot}$.

The data are presented as plots of [O/H] and [C/H] versus [Fe/H], [Si/H], and [Mg/H] in Figs. 1–3. The solid line in each figure shows the Population II sequence. It is defined by the apparent clumping of many of the stars (especially at the metal rich end) and from the figures, by the following implied abundance ratios (i.e. $[C/Fe] \sim 0.25$, $[O/Fe] \sim 0.65$, $[Mg/Fe] \sim 0.30$, and $[Si/Fe] \sim 0.35$). These ratios are similar to those found in earlier studies of the less metal poor Pop II stars (e.g. the works cited in the first paragraph of this section).

The dashed lines delineate second sequences where stars with nucleosynthetic signatures in common with the Lyman α forest gas lie. In every figure, the Cayrel et al. stars labelled 5, 30, 32, and 34 are offset from the Pop II sequence and straddle the dashed line. Other stars may also belong to this group, but either one or both of carbon, oxygen or silicon abundances are not available to confirm this possibility or they are masked by observational uncertainty especially near the observational limit. The [C-O/H] abundances of these 4 stars are plotted as a histogram in the right hand panel of Fig. 4. Note that compared to Pop II stars, these stars have reduced carbon and oxygen but enhanced silicon with respect to iron. In particular, we note that the C and O independent ratio [Si/Fe] differs by 0.2 dex between the two groups. From Fig.2 the enhanced [Si/C] ratio is ~ 0.6 . Note also that the [O/C] ratio for these stars is ~ 0.4 , similar to that of the Pop II star sequence. Based on the similarity of the observed [C-O/H] distribution and [Si/C] ratio with that of the diffuse gas, it is suggested that these 4 stars, and possibly several others, are first generation stars. Note that because the model distributions in Figure 4 begin with an assumed oxygen abundance of zero and end when the Pop II stars start to dominate, the distributions and the appropriate abundance ratios define what is referred to as first generation.

From Figs. 1–3 the first stellar generation nuclear yields [C/Mg], [O/Mg], [Si/Mg], and [Fe/Mg] are -0.4 , 0.0 , 0.2 , and -0.35 respectively, with an estimated uncertainty in each of ± 0.1 . These yields can be compared to those calculated by Heger & Woosley (2002) for a variety of Population III enrichment scenarios that are shown graphically in their Figs. 3–5. The closest fit to the first three observed ratios above is the model represented by the solid line in their Fig. 5 (i.e. high energy explosions of $12\text{--}40 M_{\odot}$ stars including exploding very massive stars ($\sim 140 - 260 M_{\odot}$) modelled with a Salpeter-like IMF. The predicted ratios [C,O,Si/Mg] are -0.31 , 0.03 , and 0.48 . Both carbon and especially silicon are over produced, but a very massive star contribution appears to be required.

3. The Chemical Evolution Model

The model employed here is similar to the one used to describe the global star formation history (H04), and it is based on the simple mass loss model (e.g. Hartwick 1976, also see Pagel 1997, and Binney & Merrifield 1998). Its novelty is a premature halting of the chemical evolution in a distributed but physically motivated way. Consider the standard one zone mass loss model of chemical evolution. Gas is slowly turned into stars while being gradually enriched in heavy elements according to a specified chemical yield, p . Simultaneously, as a result of supernova driven winds, gas with the same abundance as the gas currently forming stars is also being lost to further star formation at a rate which is proportional to the

star formation rate. The ‘effective’ yield (p_{eff}) determines the constant of proportionality, $c=(p/p_{eff})-1$.

If chemical evolution is suddenly halted before all of the gas is exhausted, a discontinuity occurs in the metallicity distribution of stars formed as well as in the lost gas, leaving a reservoir of gas with uniform composition available for later star formation. The stellar metallicity distribution can be described mathematically as the undisturbed distribution multiplied by a complementary Heaviside unit step function.

If the step function (or gas starvation function, f) is replaced with one distributed in metallicity (i.e. we round the corners of the step function), then the one zone model appears as though it contains many individually evolving boxes. In H04, for example, the complementary error function replaces the Heaviside function to be consistent with the Gaussian distribution of stoppages assumed to occur as a result of collisions among the numerous individual clumps. To provide more context for the model we give a brief summary of its application in H04.

There, by confining attention to a representative volume of the universe, the chemical evolution and star formation history associated with galaxy formation and evolution is derived from observations of stars and clusters in the Galaxy and in M31. The picture considers the anisotropic collapse of a number of star forming clumps. The gas in these clumps is assumed to have been enriched by a previous generation of star formation. The first collapse, perpendicular to the eventual rotation axis, results in collisions between low angular momentum clumps ($M_{t,blue}$) which terminates the star formation and is assumed to create the metal poor (blue) globular clusters. The stars already formed ($M_{s,blue}$) then constitute the extended metal poor halo and the gas released in the collisions ($M_{ml,blue}$) falls to the center to form the bulge. The higher angular momentum clumps ($M_{t,red}$) continue to form stars and become more metal rich until they too begin to collide as they fall along the rotation axis. These collisions again terminate star formation and give rise to the metal rich (red) globular clusters. The stars already formed ($M_{s,red}$) are released to form a metal rich spheroid population, and the gas ($M_{ml,red}$) dissipates to form the disk. Interestingly, in this picture only $\sim 20\%$ of the available baryons are required to provide an acceptable fit to the observed cosmic star formation rate density. Further, before collisions terminate star formation within the clumps, approximately half of these baryons are returned to the IGM by supernova driven winds (designated ($M_{WHIM,blue}+M_{WHIM,red}$) in H04 but renamed here M_{CGM} , the circum-galactic medium (CGM) component). Accounting for the ‘leftover’ 80% of the baryons provided one of the main motivations for the present work.

Here we assume there are a large number of star forming clumps approaching the transition to Pop II as the carbon and oxygen abundances approach $[C-O/H]\sim -3$. At this point

the gas can cool more efficiently which in turn allows low-mass Pop II stars to form more readily (e.g. Bromm & Loeb 2003). To characterize this transition we define f to be a complementary extreme value or Fisher Tippet distribution (see equation (6) below). Because the present context of the model is different from that of H04, we redefine the variables and rewrite the equations governing the chemical evolution. The conserved quantity is the total baryon mass, M_t . It is made up of 4 components: the gas contributing to star formation M_g which initially is the same as M_t , the mass in long-lived stars and/or remnants M_s , the gas lost due to supernova driven winds identified with the diffuse intergalactic medium M_{dIGM} , and the gas left to form later generations M_{LG} . From H04, with the oxygen abundance O replacing Z , M_{dIGM} replacing M_{WHIM} , and M_{LG} replacing M_{ml} the equations become:

$$M_t = M_g + M_s + M_{dIGM} + M_{LG} \quad (1)$$

$$M_g = M_t \times \exp(-(O - O_0)/p_{\text{eff}}) \times f \quad (2)$$

$$\frac{dM_s}{d\log O} = \ln 10 \times O \times M_g/p \quad (3)$$

$$M_{dIGM} = (p/p_{\text{eff}} - 1) \times M_s \quad (4)$$

and

$$\frac{dM_{LG}}{d\log O} = -M_t \times \exp(-(O - O_0)/p_{\text{eff}}) \times \frac{df}{d\log O} \quad (5)$$

where the complementary extreme value function is written

$$f = 1 - \exp(-\exp(-\log(O/O_f))/W) \quad (6)$$

For this particular problem the initial conditions are $M_g=M_t$, $M_s=0$, $M_{dIGM}=0$, $M_{LG}=0$, and $O_0=0$. The parameters O_f and W in equation (6) represent the point of inflection and the ‘width’ of the transition from one to zero of the extreme value distribution (see e.g. <http://mathworld.wolfram.com/ExtremeValueDistribution.html>).

3.1. Model Results

As shown in Table 1, 4 input parameters are required to construct a model. The constraints considered are a given true yield p for oxygen, a fit of the distribution of M_{dIGM} to the high $[O/H]$ end of the Simcoe et al. histogram (Fig. 4), and that M_{LG} be 19% of the total baryon content as required by the successful model of cosmic chemical evolution in H04. The oxygen yield was determined by combining the $[O/Fe]$ value of 0.35 from Fig. 1 with the yield assumed in H04 of $[p_Z/H] = -0.11$ (representing the iron yield) to give $[p_O/H] = 0.24$. Note that while Z was used as the model variable in H04 its observational counterpart there was always assumed to be $[Fe/H]$. The remaining 3 input parameters were then varied in order to satisfy the last two constraints resulting in the ‘nominal’ values in Table 1. In order to gauge the robustness of the results, each input parameter was varied separately by the amount tabulated, and its effects on each of the output values are also shown. The top row for each output variable shows the result of a positive variation, and the bottom row shows the negative variation. For example, the nominal value of M_{dIGM}/M_t is 0.81. If $[p_O/H]$ is increased by 0.3 M_{dIGM}/M_t remains unchanged at 0.81. If $[p_O/H]$ is decreased by 0.3, M_{dIGM}/M_t also remains unchanged at 0.81. However $[O_{eff}/H]$ is increased by 0.3, M_{dIGM}/M_t becomes 0.69 and it is increased to 0.9 for a decrease in $[O_{eff}/H]$ of 0.3 etc. In order to compare with the observations, the calculated distribution in the left hand plot of Fig. 4 was smoothed with a Gaussian kernel of width ± 0.5 and the stellar distribution with a ± 0.2 kernel to allow for observational uncertainties. The two calculated distributions appear to be quite consistent with the (limited) observations. The $[O/H]$ distribution of gas from which later stellar generations (Pop II and beyond) will form is given by equation (5).

One interesting output parameter is the value of M_s/M_t (i.e. the first generation fraction of long-lived stars and remnants, fg). Assuming that this number is representative of the universe as a whole, then $\Omega_{s,fg}/\Omega_b = 8.3 \times 10^{-4}$. If we further assume that a Magorrian-like relation holds between black hole mass and stellar mass (i.e. $M_\bullet/M_\star \sim 0.002$), then from the WMAP value of the baryon density ($\rho_b h^2 = 0.0224$, Spergel et al. 2003), one obtains $\rho_{\bullet,fg} \sim 1.0 \times 10^4 M_\odot/\text{Mpc}^3$. It is interesting to compare this number to the Yu & Tremaine (2002) determination of the same statistic at redshift zero: $2.5 \pm 0.4 \times 10^5 h_{0.65}^2 M_\odot/\text{Mpc}^3$. If the black hole seeds were formed during this first generation of star formation, then they had to have grown by ~ 25 times between then and the present time under our assumed cosmogony and implied ‘normal’ IMF. However, the nuclear yields discussed earlier suggest that the first generation IMF extends to very massive stars. This should result in additional massive black holes being formed and make the above growth factor an upper limit.

The value of the output parameter, M_{LG}/M_t , was constrained to be the baryon fraction that was determined in H04 to successfully describe the cosmic star formation history through

galaxy formation and evolution. (From Table 2 of H04 $\Omega_b = \Omega_\star + \Omega_{WHIM} + \Omega_{diffuse}$. Hence the constrained value of M_{LG}/M_t is $(\Omega_\star + \Omega_{WHIM})/\Omega_b = 0.19$ with an estimated uncertainty of ± 0.04) This number includes the mass that is lost during this process, and is the component that we now refer to as the circum-galactic medium (CGM but called WHIM in H04) in order to distinguish it from the dIGM discussed in this paper. In H04 it was found that $M_{CGM}/M_t \sim 0.09$ with a heavy element content $[\text{Fe}/\text{H}] \sim -1$. Thus, we expect there to be two gaseous components. As shown in Table 1, the dIGM is much more massive ($M_{dIGM}/M_t \sim 0.81$) and much more metal poor ($[\text{O}/\text{H}] \sim -2.9$).

If long-lived stars are formed during the Pop III phase, one may ask where are the stars with $[\text{Fe}/\text{H}] < -6$. The answer is that such stars would be exceedingly rare. In a sample of 10,000 first generation stars only 15 are predicted to have $[\text{Fe}/\text{H}] < -6$ ($[\text{O}/\text{H}] < -5.65$) based on the model distribution in Fig.4. Currently 2 stars are known with $[\text{Fe}/\text{H}] < -5$: HE 0107-5240 and HE 1327-2326 (e.g. Aoki et al. 2005). However, both of these stars show very large over abundances of carbon and so are apparently different from the stars discussed above.

4. Discussion

By identifying nucleosynthetic signatures in common, a case has been made for a connection between the diffuse IGM, as identified at high redshift with the Lyman α forest, and the first stellar generation as represented by a subsample of extremely metal poor stars. This is clearly a first step as both sets of data are small and incomplete. Some theoretical arguments suggest that only high mass stars with no long-lived luminous stellar remnants are made during the Population III phase (e.g. Bromm & Larson 2004) while others (e.g. Nakamura & Umemura 2001) have argued that the first generation IMF is bimodal with peaks at ~ 100 and $\sim 1 M_\odot$. Our result suggests that nucleosynthesis from intermediate mass stars as well as very massive stars is required to satisfy the yields found in §2.2. These nuclear yields, as well as others available but not discussed here, should allow much tighter constraints to be placed on the Pop III IMF and the accompanying ratio M_\bullet/M_\star .

Other extensions to this work are obvious. Every effort should be made to measure both oxygen and silicon in the burgeoning samples of extremely metal poor stars. Work should be concentrated on the highest gravity stars to circumvent problems with CNO mixing which occurs in the most luminous stars. In the case of the Lyman α forest observations, it would be useful to investigate the ionizing UV background to see if it could be adjusted consistently to simultaneously allow $[\text{O}/\text{C}] \sim 0.4$ and $[\text{Si}/\text{C}] \sim 0.6$ in the gas as is observed in the stellar sample.

Finally, our simple cosmogony requires two gaseous components. A circum-galactic one (CGM) arising from mass loss associated with galaxy formation and evolution, whose mass is $\sim 10\%$ of all baryons, and a diffuse IGM which contains $\sim 80\%$ of the total baryon content but which is also much more metal poor than the CGM. However, the model makes no predictions about the thermodynamic state of the gas or how it evolves. Rather, sophisticated cosmological simulations follow the evolution of these baryons which are presently considered to be in the form of a filamentary web of very low density gas (e.g. Cen & Ostriker 1999). One aspect of the model, which may be relevant to the search for local ‘missing’ baryons (e.g. Nicastro et al. 2005) and that is independent of the thermodynamic state, is that the *composition* of most of the gas may not have evolved and may still be peaked at $[C/O/H] \sim -2.9$. This could make it very difficult to observe with present instrumentation.

The author wishes to acknowledge financial support from an NSERC (Canada) discovery grant.

REFERENCES

- Akerman, C.J., Carigi, L., Nissen, P.E., Pettini, M., & Asplund, M. 2004, A&A, 414, 931
- Aoki, W., Frebel, A., Christlieb, N., Norris, J.E., Beers, T.C. et al. 2005, astro-ph/0509206
- Barklem, P.S., Christlieb, N., Beers, T.C., Hill, V., Bessell, M.S., Holmberg, J., Marsteller, B., Rossi, S., Zickgraf, F.-J., & Reimers, D. 2005, A&A, 439, 129
- Binney, J., & Merrifield, M. 1998, Galactic Astronomy, (Princeton: Princeton University Press)
- Bromm, V., & Larson, R.B. 2004, ARA&A, 42, 79
- Bromm, V., & Loeb, A. 2003, Nature, 425, 812
- Cayrel, R., Depagne, E., Spite, M., Hill, V., Spite, F., Francois, P., Plez, B., Beers, T., Primas, F., Andersen, J., et al. 2004, A&A, 416, 1117
- Cen, R., & Ostriker, J. 1999, ApJ, 514, 1
- Cowie, L.L., Songaila, A., Kim, T.-S., & Hu, E.M. 1995, AJ, 109, 1522
- Fukugita, M., & Peebles, P.J.E. 2004, ApJ, 616, 643
- Gratton, R.G., & Sneden, C.S. 1988, A&A, 204, 193
- Gratton, R.G., & Sneden, C.S. 1991, A&A, 241, 501
- Haardt, F., & Madau, P. 1996, ApJ, 461, 20

- Hartwick, F.D.A. 2004, *ApJ*, 603, 108, H04
- Hartwick, F.D.A. 1976, *ApJ*, 209, 418
- Heger, A. & Woosley, S.E. 2002, *ApJ*, 567, 532
- Honda, S., Aoki, W., Kajino, T., Ando, H., Beers, T.C., Izumiura, H., Sadakane, K., & Takada-Hidai, M. 2004, *ApJ*, 607, 474
- McWilliam, A., Preston, G.W., Sneden, C., & Searle, L. 1995, *AJ*, 109, 2757
- Nakamura, F., & Umemura, M. 2001, *ApJ*, 548, 19
- Nicastro, F., Mathur, S., Elvis, M., Drake, J., Fang, T., Fruscione, A., Krongold, Y., Marshall, H., Williams, R., & Zezas, A. 2005, *Nature*, 433, 495
- Pagel, B.E.J. 1997, *Nucleosynthesis and Chemical Evolution of Galaxies*, (Cambridge: Cambridge University Press)
- Rauch, M. 1998, *ARA&A*, 36, 267
- Ryan, S.G., Norris, J.E., & Beers, T.C. 1996, *ApJ*, 471, 254
- Simcoe, R.A., Sargent, W.L.W., & Rauch, M. 2004, *ApJ*, 606, 92
- Spergel, D.N., et al. 2003, *ApJS*, 148, 175
- Spite, M., Cayrel, R., Plez, B., Hill, V., Spite, F., Depagne, E., Francois, P., Bonifacio, P., Barbuy, B., Beers, T., et al. 2005, *A&A*, 430, 655
- Veilleux, S., Cecil, G., & Bland-Hawthorn, J. 2005, *astro-ph/0504435*
- Yu, Q., & Tremaine, S. 2002, *MNRAS*, 335, 965

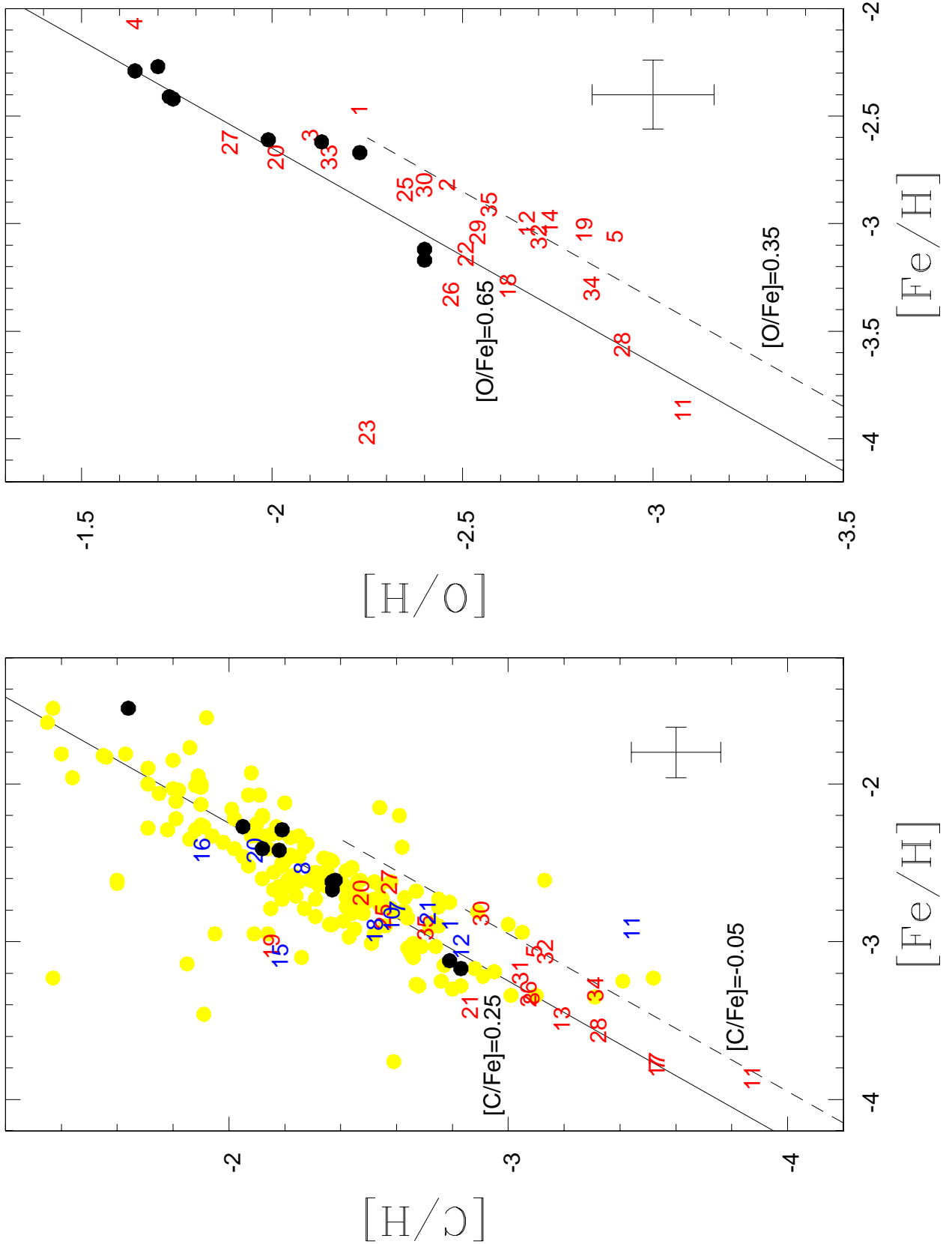


Fig. 1.— (left) $[C/H]$ vs $[Fe/H]$, (right) $[O/H]$ vs $[Fe/H]$ for extremely metal poor stars. Red numbers - data from Spite et al. (2005). Blue numbers correspond to stars in order of their appearance in the data tables of Honda et al. (2004), black dots are data from Akerman

Fig. 2.— The same as Fig. 1 except for $[\text{Si}/\text{H}]$ vs $[\text{C}/\text{H}]$ and $[\text{Si}/\text{H}]$ vs $[\text{O}/\text{H}]$

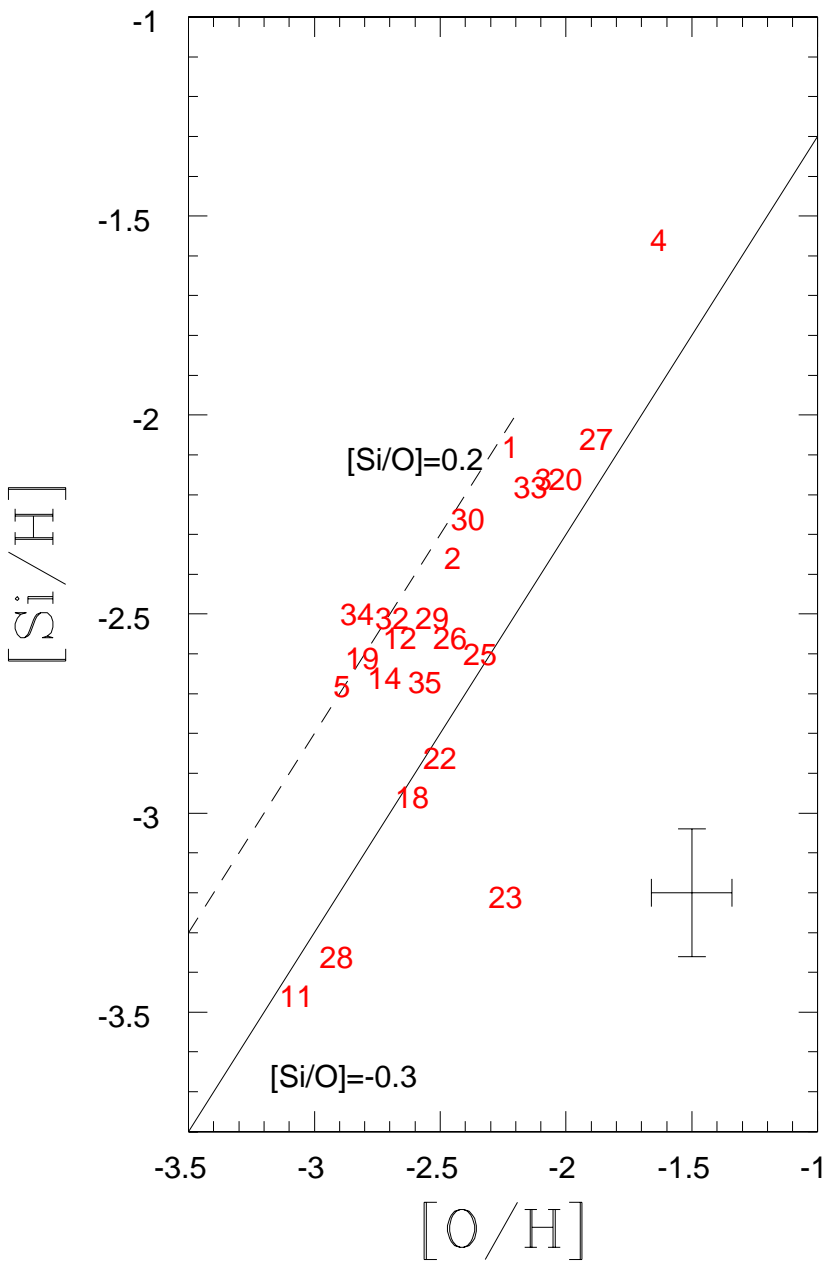
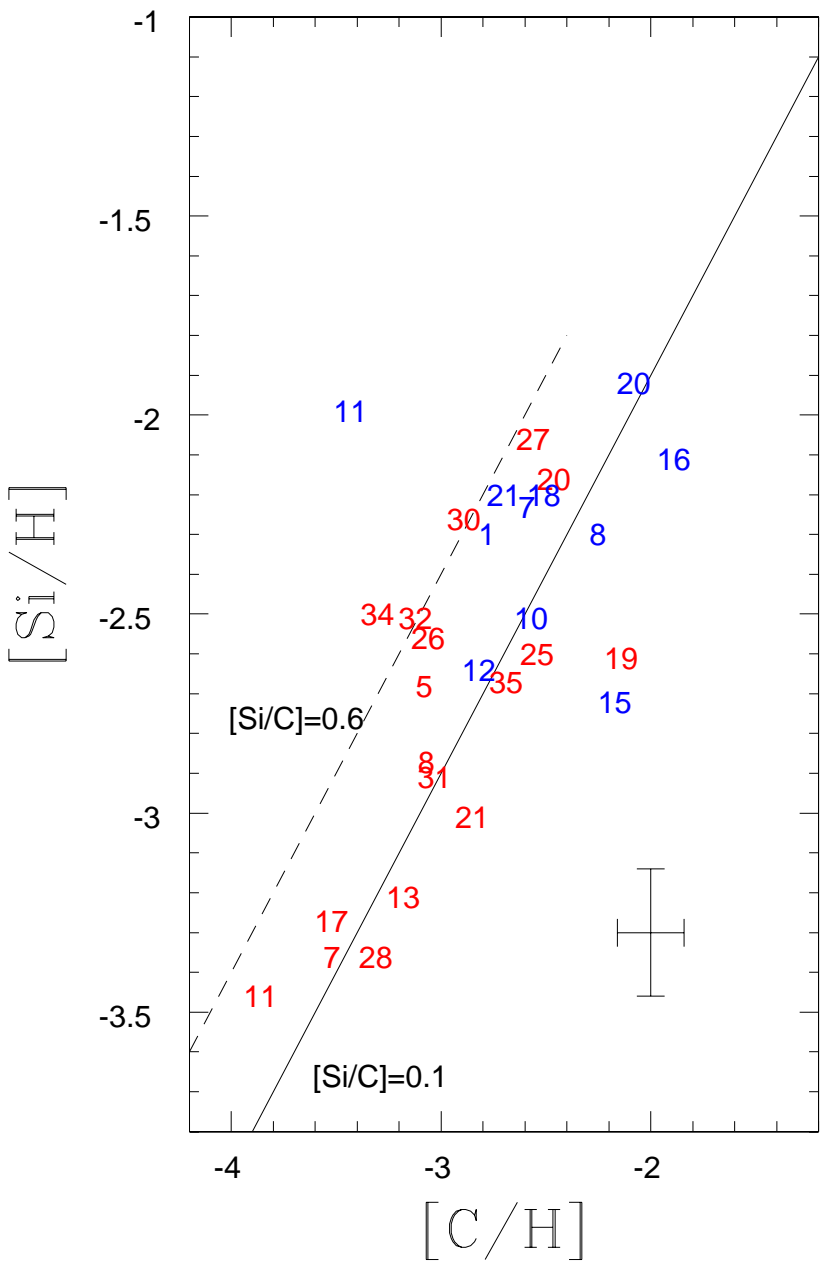
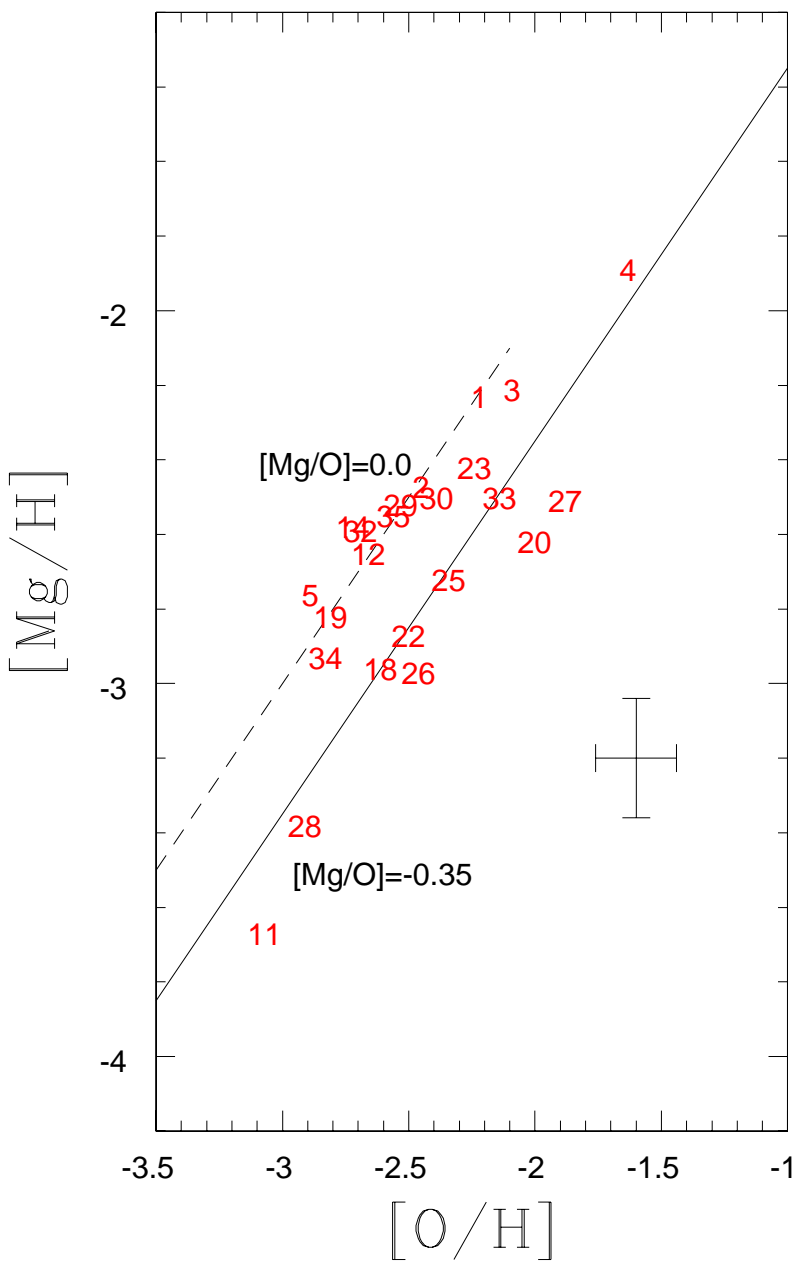
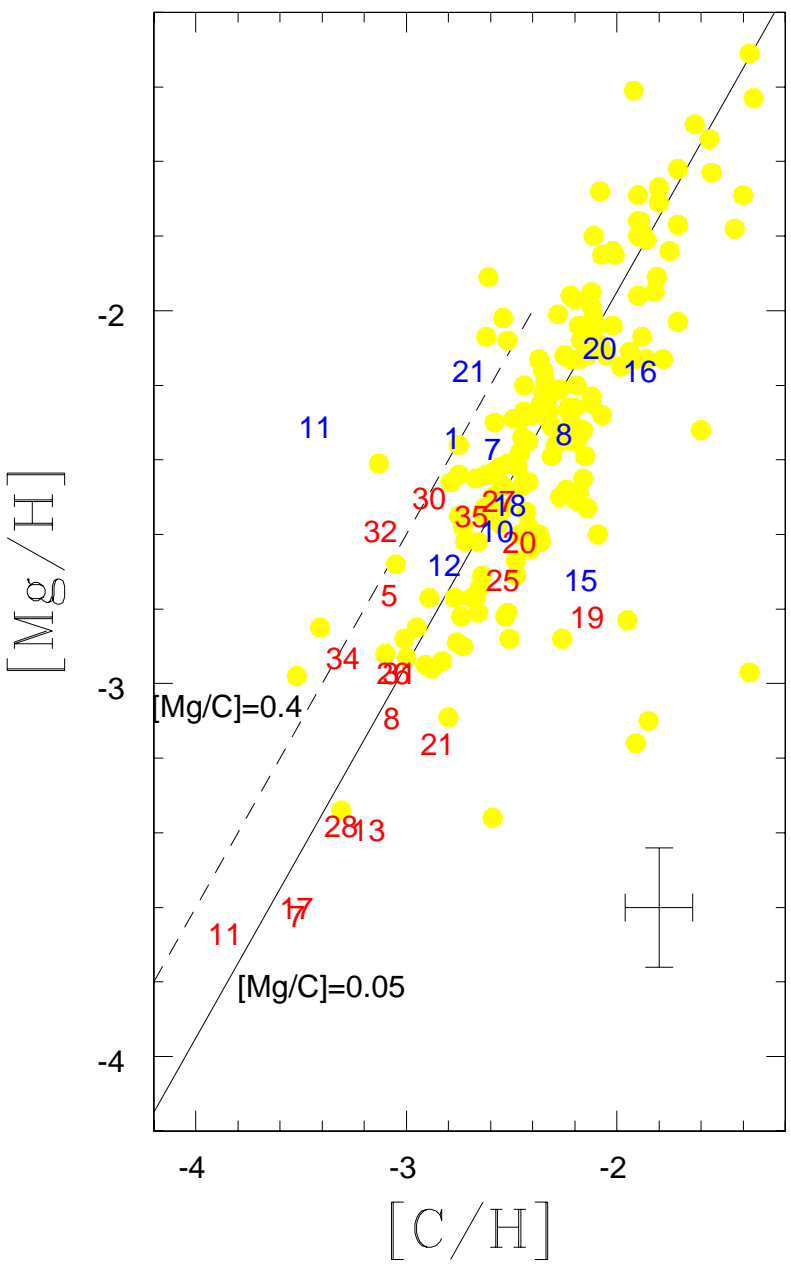


Fig. 3.— The same as Fig. 1 except for $[\text{Mg}/\text{H}]$ vs $[\text{C}/\text{H}]$ and $[\text{Mg}/\text{H}]$ vs $[\text{O}/\text{H}]$



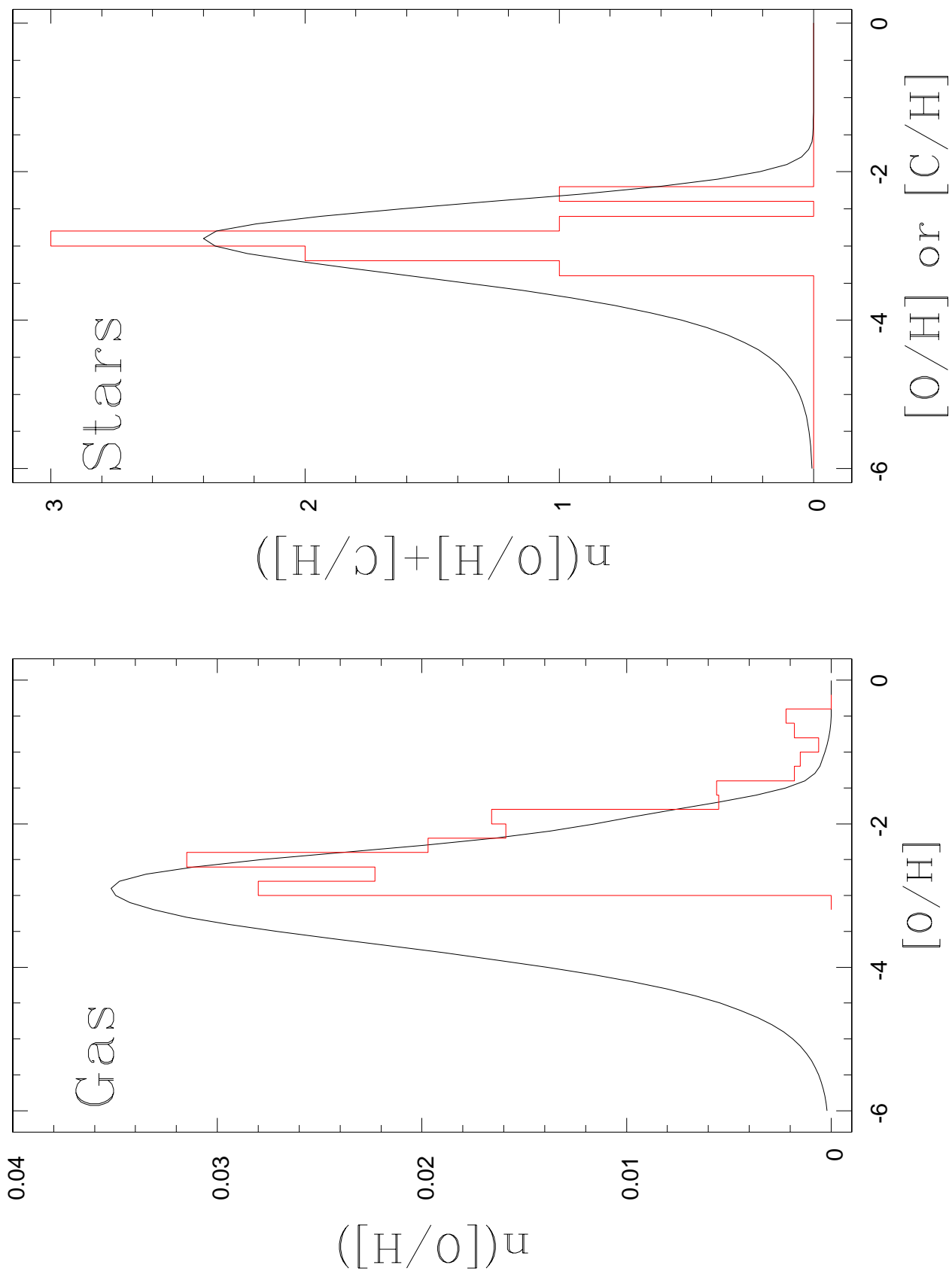


Fig. 4.— (left) A comparison of the observed abundance distribution of $[O/H]$ in the low column density Lyman α forest from Simcoe et al. (2004), with the mass loss component from the model (solid line). (right) The solid line shows the predicted distribution of $[O/H]$

Table 1. Model Parameters and Changes due to Variations in Input Parameters^a

Parameter Output	Input Nominal value	[p _O /H]	[O _{eff} /H]	[O _f /H]	1/W
		0.24 ± 0.3	−2.75 ± 0.3	−2.50 ± 0.3	1.5 ± 0.5
M _s /M _t	8.30 × 10 ^{−4}	4.16 × 10 ^{−4}	1.42 × 10 ^{−3}	9.24 × 10 ^{−4}	8.51 × 10 ^{−4}
		1.66 × 10 ^{−3}	4.63 × 10 ^{−4}	7.10 × 10 ^{−4}	7.95 × 10 ^{−4}
M _{dIGM} /M _t	0.81	0.81	0.69	0.90	0.83
		0.81	0.90	0.69	0.78
M _{LG} /M _t	0.19	0.19	0.31	0.10	0.17
		0.19	0.10	0.31	0.22
[O/H] _{max}	−2.90	−2.90	−2.70	−2.85	−2.90
		−2.90	−3.15	−2.95	−2.90

^aFor each output parameter, the upper row gives the value due to the indicated positive variations in each input parameter separately. The lower row are results from a negative variation. See text.